CARTILAGE
2022, Vol. 13(4) 200–212
© The Author(s) 2022
DOI: 10.1177/19476035221137726
journals.sagepub.com/home/CAR
SAGE

The Effect of Different Frequencies of Pulsed Electromagnetic Fields on Cartilage Repair of Adipose Mesenchymal Stem Cell–Derived Exosomes in Osteoarthritis

Yang Xu[1,2,3*], Qian Wang[1,2,3*], Xiang-Xiu Wang[1,2,3], Xiao-Na Xiang[1,2,3], Jia-Lei Peng[1,2,3], Cheng-Qi He[1,2,3], and Hong-Chen He[1,2,3]

Abstract

Background. The intra-articular injection of mesenchymal stem cell (MSC)-derived exosomes has already been proved to reverse osteoarthritic cartilage degeneration. Pulsed electromagnetic field (PEMF) has been found to regulate the biogenic function of MSCs. However, the effect of PEMF on MSC-derived exosomes has not yet been characterized. The aim of this study was to elucidate the regulatory role of different frequencies of PEMF in promoting the osteoarthritic cartilage regeneration of MSC-derived exosomes. *Methods.* The adipose tissue–derived MSCs (AMSCs) were extracted from the epididymal fat of healthy rats and further exposed to the PEMF at 1 mT amplitude and a frequency of 15, 45, and 75 Hz, respectively, in an incubator. The chondrocytes were treated with interlukin-1β (IL-1β) and the regenerative effect of co-culturing with PEMF-exposed AMSC-derived exosomes was assessed via Western blot, quantitative polymerase chain reaction, and ELISA assays. A rat model of osteoarthritis was established by anterior cruciate ligament transection (ACLT) surgery and received 4 times intra-articular injection of PEMF-exposed AMSC-derived exosomes once a week. After 8 weeks, the knee joint specimens of rats were collected for micro–computed tomography and histologic analyses. *Results.* PEMF-exposed AMSC-derived exosomes could be endocytosed with IL-1β-induced chondrocytes. Compared with the AMSC-derived exosomes alone, the PEMF-exposed AMSC-derived exosomes substantially suppressed the inflammation and extracellular matrix degeneration of IL-1β-induced chondrocytes as shown by higher expression of transcripts and proteins of COL2A1, SOX9, and ACAN and lower expression of MMP13 and caspase-1. Of these, the 75-Hz PEMF presented a more significant inhibitive effect than the 15-Hz and 45-Hz PEMFs. Furthermore, the intra-articular injection of 75-Hz PEMF-exposed exosomes could obviously increase the number of tibial epiphyseal trabeculae, lead to a remarkable decrease in Osteoarthritis Research Society International score, and upregulate the COL2A1 and ACAN protein level of the degenerated cartilage. *Conclusion.* The present study demonstrated that PEMF stimulation could effectively promote the regeneration effects of AMSC-derived exosomes on osteoarthritic cartilage. Compared with other frequency parameters, the PEMF at a frequency of 75 Hz showed a superior positive effect on AMSC-derived exosomes in suppressing the IL-1β-induced chondrocyte inflammation and extracellular matrix catabolism, as well as the osteoarthritic cartilage degeneration.

Keywords

adipose mesenchymal stem cell, exosomes, pulsed electromagnetic fields, osteoarthritis, cartilage repair

Introduction

Osteoarthritis (OA) is a prevalent chronic inflammatory disease worldwide, with a strong impact on individual health.[1-4] OA is characterized by pathology involving the whole joint, including cartilage degradation, bone remodeling, osteophyte formation, and synovial inflammation, leading to pain, stiffness, swelling, and loss of normal joint function.[5-7] Although the administration of various kinds of stem cells has been demonstrated for effective cartilage repair,[8] alternative clinical approaches have been also

[1]Rehabilitation Medicine Centre, West China Hospital, Sichuan University, Chengdu, P.R. China
[2]School of Rehabilitation Sciences, West China School of Medicine, Sichuan University, Chengdu, P.R. China
[3]Rehabilitation Medicine Key Laboratory of Sichuan Province, Chengdu, P.R. China
*Yang Xu and Qian Wang contributed equally to the work.

Corresponding Author:
Hong-Chen He, Rehabilitation Medicine Centre, West China Hospital, Sichuan University, Chengdu 610041, Sichuan, P.R. China.
Email: hxkfhhc@126.com

investigated to overcome the current limitations of cell-based therapies, such as immune responses, deterioration of stem cells' intrinsic activity, or variation by age of cell donors.[9-11]

In this case, exosomes could deliver a variety of biological signals including protein, cytokines, and microRNA (miRNA), which are derived from the source stem cells. It could be reasonably expected that exosome is an alternative off-the-shelf therapeutic option to replace conventional stem cell products.[12-14] The literature review has shown that the intra-articular injection of MSC-derived exosomes could promote the cartilage regeneration and reduce the inflammatory response and immune regulation. However, the insufficient secretion of MSC-derived exosomes and the heterogeneity of exosome-capsulated miRNAs have become the major bottleneck, restricting its clinical transformation.[15] To exert its best regenerative repair, it is of necessity to regulate the biological function of MSC-derived exosomes.[16-19]

Pulsed electromagnetic field (PEMF) has been clinically used in the treatment of OA.[20] Also, PEMF treatment increased bone and cartilage formation, and decreased bone and cartilage resorption in the MIA (monoiodoacetic acid)-induced OA rat model.[21] Notably, it has been found that the PEMF can regulate the biological function of MSCs in the cartilage regeneration, such as enhancing the inhibitory effect on nitric oxide synthase (NOS) activity and preserving the anabolic activity.[22-24] Furthermore, MSC paracrine signaling has been found to be affected by PEMF stimulation, hence representing a manner of promoting regeneration of MSCs in an inflammatory joint environment.

However, the effect of PEMF with different frequencies on MSC-derived exosomes in osteoarthritic cartilage has still been unknown. Therefore, this study aimed to explore the regulatory effect of PEMF with different frequencies on osteoarthritic cartilage regeneration of adipose tissue MSC-derived exosomes through *in vivo* and *in vitro* experiments. The finding will open up a new direction for enhancing the therapeutic effect of MSC-derived exosomes on OA.

Materials and Methods

Ethics Statement

This study was conducted under the approval of the Animal Ethical Committee of West China Hospital, Sichuan University. All animal care and surgical techniques strictly complied with the Declaration of Helsinki.

In Vitro Study

Isolation and characterization of rat adipose mesenchymal stem cells. Adipose mesenchymal stem cells (AMSCs) were isolated from 3-week-old healthy Sprague-Dawley rats' epididymal fat ($n = 2$, provided by the Chengdu Dossy Experimental Animals Company) according to the previous literature.[25] Low-glucose Dulbecco's modified Eagle's medium (DMEM) (Gibco, USA) supplemented with 10% fetal bovine serum (FBS; Cell-Box, Australia) containing adipose cells was cultured at 37 °C in 5% CO_2 cell culture incubator. The medium was replaced for the first time after 48 hours and was replaced every 2 to 3 days afterward. Passage 3-6 (P3-P6) cells were used for subsequent experiments. For phenotype characterization, AMSCs were stained with rabbit anti-rat polyclonal antibodies CD34, CD44, CD90, and CD45 (Abcam Inc., USA) and analyzed by flow cytometry (BD FACSCanto™, USA).

For determining the multipotent differentiation capabilities of rat AMSCs, including osteogenic, adipogenic, and chondrogenic differentiation, AMSCs were cultured in the following medium types: (1) osteogenic differentiation medium—high-glucose DMEM, 10% FBS, 50 μg/ml ascorbic acid, 10 mM β-glycerophosphate, 10 nM dexamethasone, 100 U/ml streptomycin, and 100 U/ml penicillin (Cyagen Biosciences Inc., Guangzhou, China); (2) adipogenic differentiation medium—high-glucose DMEM, 10% FBS, 0.1 mmol/l 3-isobutyl-1-methylxanthine, 10 μg/ml insulin, 10 nM dexamethasone, 50 μg/ml indomethacin, 100 U/ml streptomycin, and 100 U/ml penicillin (Cyagen Biosciences Inc., Guangzhou, China); and (3) chondrogenic differentiation medium—high-glucose DMEM, 50 μg/ml ascorbic acid, 100 nM dexamethasone, 1 mM sodium pyruvate, 40 μg/ml proline, 100 U/ml streptomycin, 100 U/ml penicillin (Cyagen Biosciences Inc., Guangzhou, China), 10 ng/ml TGFβ3 (Cyagen Biosciences Inc., Guangzhou, China), ITS + premix (final concentrations, 6.25 μg/ml bovine insulin, 6.25 μg/ml transferrin, 6.25 μg/ml selenous acid, 5.33 μg/ml linoleic acid, and 1.25 mg/ml bovine serum albumin) (Cyagen Biosciences Inc., Guangzhou, China). The induction medium was changed every 3 days. On day 14, cells were fixed and stained with Alizarin Red S for osteocytes, Oil Red O for adipocytes, and Alcian Blue for pellet culture chondrocytes (Cyagen Biosciences Inc., Guangzhou, China).

PEMF stimulates MSC-derived exosomes. Rat MSCs (P3-P6) were cultured in low-glucose DMEM (Gibco, USA) when cell confluence reached 80% to 90%. The custom-designed PEMF exposure system comprises a waveform signal generator (DG1022U; RIGOL, Suzhou, China), an adjustable switching power supply (MS-605D; Maisheng, Dongguan, China), a power amplifier, and Helmholtz coils with a 3-coil array. The signal generator can send electromagnetic fields with a pulse duration of 300 μs, amplitude of 1 mT, and adjustable frequency. The magnetic field intensity was measured using a hand-held gaussmeter (HT201; Hengtong, Shanghai, China). Twelve 10 cm cell culture plates can be

Figure 1. PEMF modulates AMSC-derived exosomes in the incubator.
PEMF = pulsed electromagnetic field; AMSC = adipose tissue–derived MSC.

contained inside the cylindrical electromagnetic coil seal, embedded in the middle of the constant temperature incubator. MSC cells were cultured in pure low-glucose DMEM before being exposed to PEMF for 30 minutes at 0, 15, 45, and 75 Hz (**Fig. 1**), respectively, and conditioned media from pellet culture were collected 24 hours post-PEMF exposure and pooled for later use. Exosomes were isolated and purified by ultracentrifugation and identified and counted by the NTA (Nanoparticle Tracking Analysis) machine.

Isolation and characterization of MSC-derived exosomes. MSCs were cultured in pure low-glucose DMEM for 48 hours to collect the conditioned medium. The supernatant was then centrifuged at 120,000*g* at 4 °C for 90 minutes using a 45 Ti rotor (Beckman Coulter, USA). The resulting pellets were washed and resuspended in phosphate-buffered saline (PBS), followed by centrifugation at 120,000*g* at 4 °C for 90 minutes.

The exosome morphology was observed under 100-kV transmission electron microscopy (TEM; HITACHI H-7000FA, Japan). The particle size distribution of exosomes was analyzed by Zetaview (Particle Metrix, Germany). Antibodies against CD9 (Abcam, UK) and TSG101 (Abcam) were used to identify the protein-level expressions by Western blot.

Primary culture of chondrocytes and in vitro *model of OA-like chondrocytes.* Rat chondrocytes were isolated from 1-week-old Sprague-Dawley rats' ribs (n = 2, provided by the Chengdu Dossy Experimental Animals Company) according to the previous literature.[26] The resultant cells were

Table 1. Primer Sequences and Mapleton Sizes for Quantitative Polymerase Chain Reaction.

Genes	Primer Sequence (5′-3′)
MMP13	F: 5′-AGCAGGTTGAGCCTGAACTGT-3′ R: 5′-GCAGCACTGAGCCTTTTCACC-3′
COL2A1	F: 5′-GCCCAACTGGCAAACAAGGAGAC-3′ R: 5′-GCAGGGCCAGAAGTACCCTGATC-3′
ACAN	F: 5′-GGCTTCCCACCGTCCCAGCAG-3′ R: 5′-GAAGTGTCTGTGCTGCCTGTGAA-3′
Caspase1	F: 5′-CTTGGAAATAGCTCCCAGAA-3′ R: 5′-CATTTGGGAACTTCTCATCC-3′
SOX9	F: 5′-GCGTATGAATCTCCTGGACC-3′ R: 5′-GCGGCTGGTACTTGTAATCC-3′
GAPDH	F: 5′-CCTGGAGAAACCTGCCAAGTAT-3′ R: 5′-TAGCCCAGGATGCCCTTTAGT-3′

cultured with DMEM/F-12 medium containing 10% FBS, 100 U/ml penicillin, and 100 U/ml streptomycin (Gibco). The medium was changed every 3 days. For all experiments described, the chondrocytes in monolayer culture were used between passages 2 and 4.

For the *in vitro* model of OA-like chondrocytes, chondrocytes were induced to express an OA-like phenotype by interleukin (IL)-1β treatment (Cyagen Biosciences Inc.). Briefly, IL-1β (10 ng/ml) was added to the chondrocyte's medium for 24 hours.

MSC-derived exosome uptake in vitro. Exosomes were labeled using the red fluorescent dye 3,3′-dioctadecyloxacarbocyanine perchlorate (DiO) according to the manufacturer's instructions (Cyagen Biosciences Inc.). Excess dye from the labeled exosomes was removed by ultracentrifugation at 100,000*g* for 1 hour at 4 °C, and the exosome pellets were washed 3 times by PBS. The final pellets were resuspended in PBS. Exosomes were co-cultured with rat chondrocytes at a concentration of 1×10^8 particles/ml in a serum-free medium at 37 °C for 24 h and then fixed with 4% paraformaldehyde. The nuclei were stained with 4′,6-diamidino-2-phenylindole (DAPI). The uptake of exosomes was observed using a Celigo® Image Cytometer.

Real-time RT-qPCR. Total RNA was extracted from cells using the Total Exosome Isolation Reagent (Invitrogen, USA), followed by reverse transcription to generate the first-strand cDNA using the PrimeScript RT reagent Kit (Takara, Japan) according to the manufacturer's protocol. Quantitative polymerase chain reaction (PCR) was performed using the SYBR Green PCR mix (Takara, Japan) on a Bio-Rad CFX Connect real-time system (Bio-Rad, USA). Primer sequences are shown in **Table 1**. GAPDH was regarded as a reference gene. The PCR reaction experiment of each sample was repeated 3 times, and the reverse transcription (RT)-PCR data were analyzed by the $2^{-\Delta\Delta Ct}$ method.

Enzyme-linked immunosorbent assay. The COL2A1 level was measured by enzyme-linked immunosorbent assay (ELISA) using the COL2A1 ELISA kit (R&D, Shenzhen Jingmei Ltd., China) according to the manufacturer's instructions. Control buffer and chondrocyte samples were added into wells of ELISA plates containing antibody COL2A1 and then were incubated for 2 hours at room temperature. After washing, 100 µl of the secondary antibody–conjugated horseradish peroxidase (HRP) was added to each well and incubated for 2 hours. It was then washed again, and 100 µl of treated TMB (4,4'-Diamino-3,3',5,5'-tetramethylbiphenyl) was added into each well and incubated for 15 minutes without light. The reaction was stopped with lNH2SO4 and the absorbance was measured at 450 nm.

Western blot. Passage 2-4 chondrocytes were used for protein extraction. Briefly, chondrocytes were washed with PBS 3 times and lysed with radioimmunoprecipitation assay (RIPA) lysis buffer (Beyotime, China) supplemented with 1 mM protease inhibitor cocktail and 1 mM phosphatase inhibitor cocktail (Thermo, USA). The mixture was homogenized and lysed on ice and centrifuged at 12,000*g* for 30 minutes at 4 °C. The resulting supernatant was collected. Protein concentration was determined by the bicinchoninic acid (BCA) method (Beyotime). The same amount of protein sample was electrophoresed and transferred to the polyvinylidene fluoride (PVDF) membrane (Millipore, USA). The membrane was blocked with 5% skim milk for 1 hour at room temperature and incubated at 4 °C overnight with the primary antibody against SOX9 (Abcam), Casp1 (Abcam), IL-1β (Abcam), and β-actin (Abcam). After washing, the membrane was incubated with secondary antibodies (Abcam) at room temperature for 1 hour. The protein bands were exposed using ChemiDoc MP (Bio-Rad). Integrated density for protein bands was determined using Image J (National Institutes of Health, USA).

In Vivo *Study*

The rat model of OA and experimental design. Thirty-nine 8-week-old male SD rats (provided by the Chengdu Dossy Experimental Animals Company) were anesthetized with 2.5% to 3% isoflurane. Twenty-seven rats underwent unilateral anterior cruciate ligament transection (ACLT) (Each rat was anesthetized with isoflurane, and after being shaved and disinfected, the right knee joint was exposed through a medial parapatellar approach. The patella was dislocated laterally and the knee was placed in full flexion followed by ACL transaction with micro-scissors.) to produce the OA change of the knee. Rats in the blank group ($n = 6$) received no intervention, and rats in the sham group ($n = 6$) underwent joint puncture only. Four weeks later, intra-articular injection of MSC-derived exosomes (1×10^9 particles/1 ml) was performed in the OA rats once a week ($n = 7$, OA +

EXO group; $n = 7$, OA + 75 Hz EXO group) (AMSC-derived exosomes exposed to PEMF were injected with the same concentration), while intra-articular injection of 10 μl of normal PBS was performed in the OA + PBS group ($n = 7$). At 8 weeks after surgery, the knee joint specimens of rats were collected for histologic analysis and PCR. All the *in vivo* data for cartilage repair were obtained from the same set of animals.

Micro-CT imaging study. At 8 weeks of treatment, rats were sacrificed and the distal part of the femur and the proximal part of the tibia were cut with a blunt scissor to acquire knee joint tissues. Muscles and ligaments were completely dissected, and bone and cartilage were scanned with a micro–computed tomography (CT). The scanning time for the micro-CT scanner was adjusted to 4 minutes with a setting of 80 kVp, 100 μA, and 20 calibrations. Axial and transaxial fields of view of 20 mm were acquired. Micro-CT images were also reconstructed into a 3-dimensional (3D) image to show the OA changes.

Histological staining and immunohistochemistry. At 8 weeks of treatment, the rats were sacrificed and articular cartilage samples were collected. After fixation with paraformaldehyde for 24 hours and decalcified for 21 days in 10% ethylenediaminetetraacetic acid (EDTA; pH 7.4), tissues were embedded in paraffin and sectioned into a 5-μm-thick section. The serial sections were obtained from the medial and lateral compartments at 200-μm intervals. The selected sections were deparaffinized in xylene, rehydrated through a graded series of ethanol washes, and followed by hematoxylin and eosin (H&E). The degree of cartilage degeneration was assessed on the medial and lateral tibial plateau joint with the Osteoarthritis Research Society International (OARSI) score. Histologic scoring is performed on the 3 most severely affected consecutive sections (at 200 mm intervals) using the coronal sectioning method. The values for each parameter (cartilage matrix loss width, cartilage degeneration score, total cartilage degeneration width, significant cartilage degeneration width, osteophytes, etc.) are then averaged across the 3 scored sections per knee joint.[27]

For immunohistochemistry (IHC), the deparaffinized sections were soaked in EDTA (pH 9.0) for antigen retrieval by a microwave method. The sections were placed in a 3% hydrogen peroxide solution and incubated at room temperature for 25 minutes in the dark, followed by blocking with 3% bovine serum albumin at room temperature for 30 min. Then, the sections were incubated with primary antibodies COL2A1 (Abcam) and ACAN (Abcam) at 4 °C overnight, followed by the secondary antibody (Abcam) at room temperature for 60 minutes the next day. After extensive washing, 3,3′-diaminobenzidine (DAB)-peroxidase substrate and hematoxylin solution (Servicebio, China) were added.

Statistical Analysis

Data are expressed as mean ± standard deviation (SD). Repeated measures were analyzed by repeated-measures analysis of variance (ANOVA) with Bonferroni *post hoc* analysis. The other data were analyzed by 1-way ANOVA with Bonferroni *post hoc* analysis. All statistical analyses were performed using the IBM SPSS software (SPSS Statistics V22; IBM Corporation, USA). P values <0.05 were considered statistically significant.

Results

Characterization of AMSCs and AMSC-Derived Exosomes

The AMSCs were extracted from the rat adipose tissue. Flow cytometry analysis showed that AMSCs were positive for mesenchymal markers, including CD44 and CD90, but negative for CD34 and CD45 (**Fig. 2A**). In addition, the multilineage differentiation potential of AMSCs was demonstrated by Alizarin Red staining, Oil Red O staining, and Alcian Blue staining (**Fig. 2B**).

For exosome preparation, 200 ml of AMSC-conditioned medium was centrifuged, and 50 μg of exosomes can be purified. The dynamic light-scattering measurement indicated that the mean size of AMSC-derived exosomes was 164 nm (**Fig. 2C**). TEM showed that the exosomes exhibited an oval shape (**Fig. 2D**). For the Western blot of exosome surface markers, 20 μg of AMSCs or exosomes was loaded onto sodium dodecyl sulfate polyacrylamide gel electrophoresis (SDS-PAGE). Western blot analysis indicated that these vesicles displayed exosome surface markers, including CD9 and TSG101 (**Fig. 2E**).

PEMF-Exposed AMSC-Derived Exosomes Could Enter Chondrocytes

To investigate whether PEMF-exposed AMSC-derived exosomes could enter chondrocytes through co-culture, exosomes stained with DiO were co-cultured with chondrocytes, and 24 hours later chondrocytes were observed under a fluorescence microscope. The images showed that when co-cultured with chondrocytes, PEMF-regulated AMSC-derived exosomes gathered inside the chondrocytes, and fluorescence was observed in the whole chondrocytes (**Fig. 3A**), suggesting that some exosomes endocytosed into the chondrocytes.

PEMF Enhanced the Inhibitory Effect of AMSC-Derived Exosomes on IL-1β-Induced Chondrocyte Inflammation

Next, to evaluate whether PEMF at different frequencies could modulate the effect of AMSC-derived exosomes on

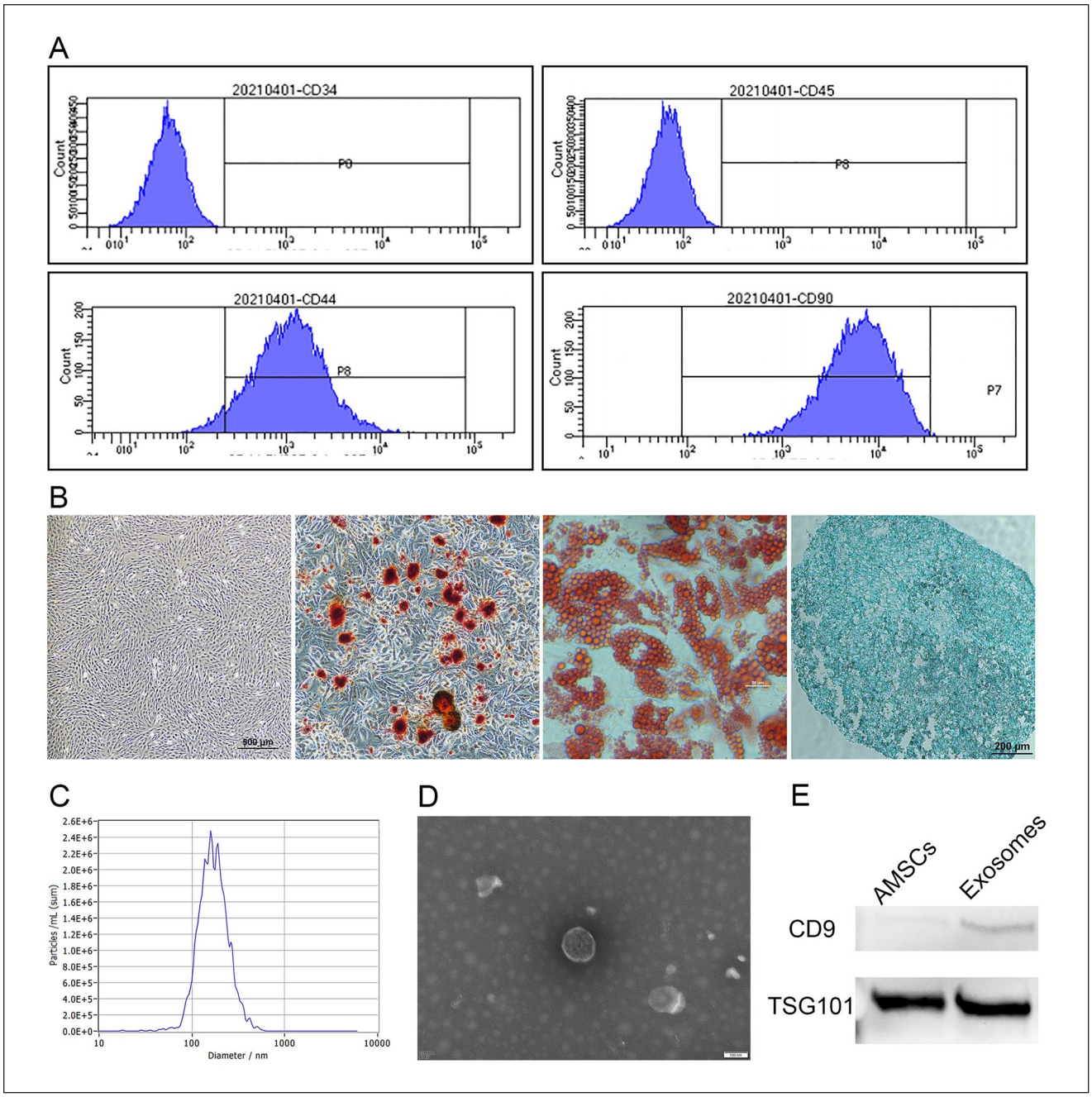

Figure 2. Characterization of AMSCs and AMSC-derived exosomes. (**A**) Flow cytometry analysis showed that AMSCs were positive for mesenchymal markers, including CD44 and CD90, but negative for CD34 and CD45. (**B**) The image of AMSCs, and the multilineage differentiation potential of AMSCs was demonstrated by Alizarin Red staining, Oil Red O staining, and Alcian Blue staining. (**C**) The dynamic light-scattering measurement indicated that the mean size of AMSC-derived exosomes was 164 nm. (**D**) TEM showed that the exosomes exhibited an oval shape (scale bar = 100 nm). (**E**) Western blot analysis indicated that these vesicles displayed exosomal surface markers, including CD9 and TSG101.
AMSC = adipose tissue–derived MSC; TEM = transmission electron microscopy.

IL-1β-induced chondrocyte inflammation, the expressions of common inflammation factors in OA (matrix metalloproteinase 13 [MMP13], caspase-1, and IL-1) were assessed in IL-1β-treated chondrocytes. As shown in **Figure 3B**, IL-1β treatment significantly upregulated MMP13 ($P < 0.05$) and caspase-1 ($P < 0.01$) mRNA expressions; however, the treatment of MSC-derived exosomes and PEMF-exposed AMSC-derived exosomes (1×10^8 particles/ml) significantly

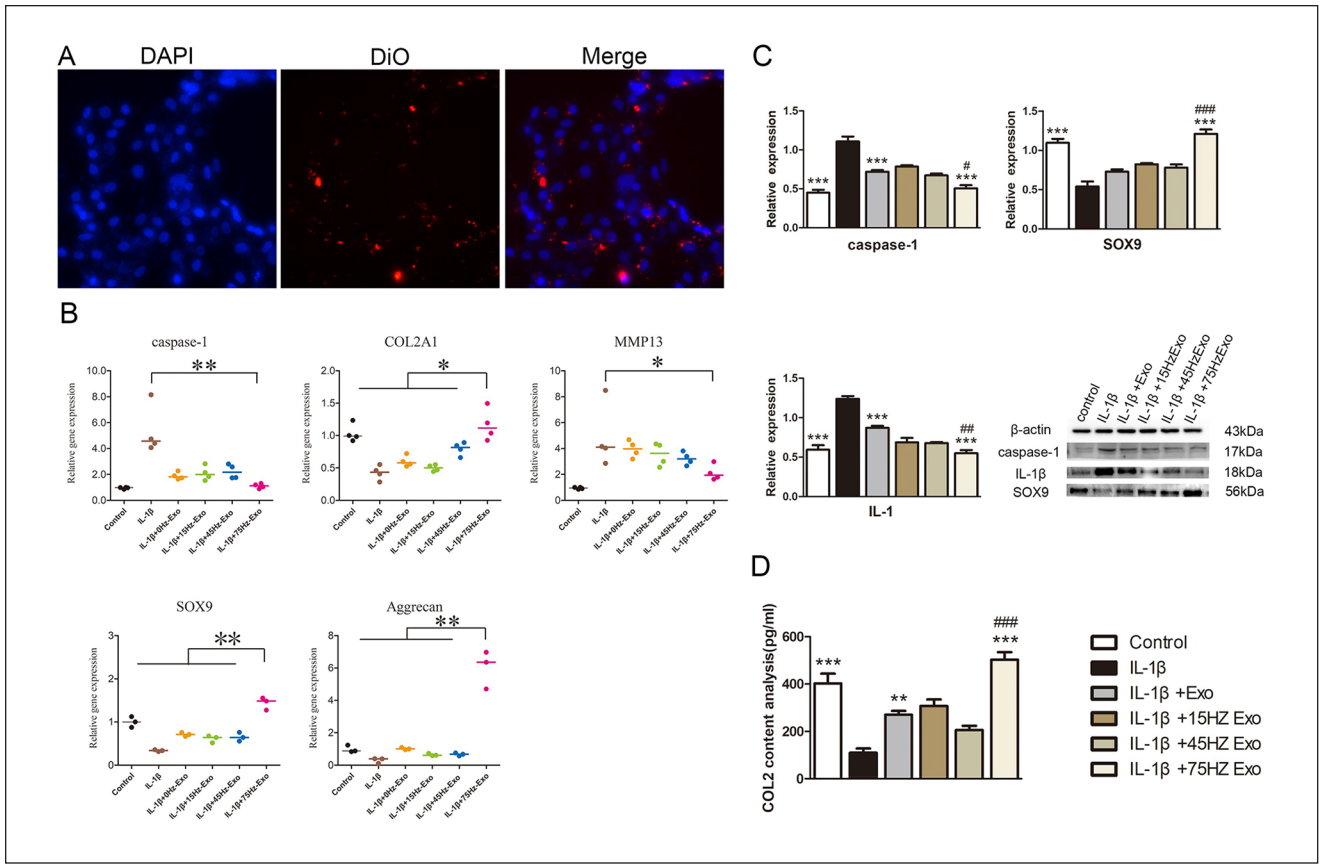

Figure 3. PEMF-regulated AMSC-derived exosomes attenuated IL-1β-induced downregulation of anabolic markers and upregulation of catabolic markers in cartilage degradation. **(A)** Immunofluorescence staining of chondrocytes and AMSC-derived exosomes (DiO) showed that exosomes gathered inside the chondrocytes (20x). **(B-D)** All experiments were repeated independently for at least 3 biological replicates. In the *in vitro* model of chondrocyte degeneration, PCR (**B**), ELISA (**C**), and Western blot (**D**) assays were performed to determine the mRNA and protein levels of ACAN, COL2A1, SOX9, MMP13, IL-1, and caspase-1. **<0.01, ***<0.001, compared with the IL-1β group. #<0.05, ##<0.01, ###<0.001, compared with the OA + EXO group.
PEMF = pulsed electromagnetic field; AMSC = adipose tissue–derived MSC; DiO = 3,3′-dioctadecyloxacarbocyanine perchlorate; PCR = polymerase chain reaction; IL = interleukin.

attenuated IL-1β-induced changes in the expression of these genes ($P < 0.01$ except for MMP13 in OA + EXO group). And PEMF-exposed AMSC-derived exosomes had a substantially better attenuation effect on IL-1β-induced chondrocytes than AMSC-derived exosomes. Among all parameters, the 75-Hz PEMF-exposed MSC-derived exosomes presented a higher inhibitive effect on the IL-1β-induced upregulation of MMP13 and caspase-1 mRNA expressions than 15 and 45 Hz ($P < 0.01$)

Western blot (**Fig. 3C**) also demonstrated that IL-1β induction significantly upregulated the expression of IL-1 ($P < 0.01$) and caspase-1 ($P < 0.01$) proteins. And the treatment of AMSC-derived exosomes (1×10^8 particles/ml) on chondrocytes significantly attenuated this overexpression ($P < 0.01$). Also, PEMF substantially enhanced the downregulation effect of AMSC-derived exosomes on IL-1 and caspase-1 protein expressions, while PEMF at a frequency of 75 Hz performed better than the 2 other parameters ($P < 0.01$, $P < 0.01$).

PEMF Promoted the Suppression Effect of AMSC-Derived Exosomes on IL-1β-Induced Chondrocyte Matrix Degeneration

In addition, to investigate whether PEMF could modulate the effect of AMSC-derived exosomes on IL-1β-induced reduction in chondrocyte matrix synthesis, the expressions of common anabolic markers (COL2A1, ACAN, and SOX9) were assessed in IL-1β-treated chondrocytes. As shown in **Figure 3B**, IL-1β treatment significantly downregulated COL2A1 ($P < 0.05$), ACAN ($P < 0.01$), and SOX9 ($P < 0.01$) mRNA expressions; however, AMSC-derived exosomes and PEMF-exposed AMSC-derived exosomes (1×10^8 particles/ml) significantly attenuated IL-1β-induced changes in the expression of these genes ($P < 0.01$ except for COL2A1 in OA + EXO group). Meanwhile, the exposure of PEMF substantially enhanced the upregulation effect of AMSC-derived exosomes on COL2A1 ($P < 0.05$),

ACAN ($P < 0.01$), and SOX9 ($P < 0.01$) mRNA expressions. Also, compared with PEMF at 15 and 45 Hz, the 75-Hz PEMF-exposed AMSC-derived exosomes upregulated the expression of COL2A1 ($P < 0.05$), ACAN ($P < 0.01$), and SOX9 ($P < 0.01$) mRNA to a higher level.

In addition, ELISA (**Fig. 3D**) also demonstrated that AMSC-derived exosomes (1×10^8 particles/ml) significantly attenuated IL-1β-induced low expression of COL2A1 proteins ($P < 0.01$). Meanwhile, ELISA (**Fig. 3D**) and Western blot (**Fig. 3C**) displayed that PEMF enhanced the upregulation effect of AMSC-derived exosomes on COL2A1 ($P < 0.01$) and SOX9 ($P < 0.01$) protein expressions, of which the 75-Hz PEMF performed better than the 15- and 45-Hz PEMFs ($P < 0.01$).

PEMF-Stimulated AMSC-Derived Exosomes Alleviate Cartilage Damage in ACLT-Induced Experimental OA Rats

Given that OA was always accompanied by cartilage defects, we hypothesized that AMSC-derived exosomes exposed to PEMF could alleviate the progression of OA via inducing chondrocyte matrix synthesis. In support of this hypothesis, an OA rat model was established with the ACLT method. According to the present *in vitro* studies, the 75-Hz PEMF was supposed to have better promoting effect on AMSC-derived exosomes in cartilage repair. Hence, the animals were randomly divided into 6 groups: blank group, sham group, OA group, OA + PBS group, OA + EXO group, and OA + 75 Hz EXO group. Rats in the last 2 groups took intra-articular injections with exosomes (40 μl; 1×10^9 particles/ml; once a week) for 4 weeks.

Eight weeks after the model was established, the knee joint specimens of animals were collected for micro-CT imaging studies (**Fig. 4A**) and H&E staining (**Fig. 4B**). The micro-CT images displayed that in the blank and sham groups, the transverse section of the epiphyseal proximal tibia had a large number of trabeculate and a higher bone density. While in the OA group the number of bone trabeculae reduced, the OA + EXO and OA + 75 Hz EXO groups restrained this reduction. In addition, the staining showed that in the sham group, the articular cartilage was clear with a smooth and intact surface. In the OA group, the surface of the articular cartilage was rough and fractured. Part of the subchondral bone was exposed, and the synovium exhibited hyperemia and significant hyperplasia. Compared with the blank and sham group, the cartilage layer of the OA group was lightly stained and thinner. The subchondral bone was thickened with disordered structure and formation of multiple osteophytes, suggesting the OA model was successfully established. The OA + EXO and OA + 75 Hz EXO groups exhibited a few defects and fractures on the cartilage surface, suggesting that exosomes attenuated cartilage damage in OA animals.

The OARSI scores of the knee joint specimens were significantly higher in the OA group than in the sham group (4.4 ± 0.3 vs. 0.3 ± 0.2, $P < 0.01$). The intra-articular injection of AMSC-derived exosomes significantly reduced the OARSI scores compared with the OA group (2.8 ± 0.2 and 2.4 ± 0.4 vs. 4.4 ± 0.3, $P < 0.01$) (**Fig. 4C**). The score was mainly decided according to the cartilage matrix loss and cartilage degeneration observed in the frontal sections.[25]

To further clarify the relationship between COL2A1, ACAN, and extracellular matrix (ECM), IHC staining of COL2A1 and ACAN was performed in the knee cartilage layer of the *in vivo* knee joint OA model. The results showed that with the increase in COL2A1 and ACAN protein expression in chondrocytes, they were also found to be increased in the ECM (**Fig. 4D**). In addition, the expression of COL2A1 and ACAN in the chondrocytes and ECM was higher in the OA + EXO group and OA + 75 Hz EXO group than in the OA group with no statistical significance.

Discussion

In the present study, we investigated the regulatory effect of PEMF with different frequencies on osteoarthritic cartilage regeneration of AMSC-derived exosomes. The *in vitro* study showed that the PEMF-stimulated AMSC-derived exosomes significantly attenuated the ECM degeneration and inflammation in the IL-1β-induced chondrocytes. Of these, the 75-Hz PEMF exposure exhibited a superior effect than 15- and 45-Hz PEMFs. Furthermore, the 75-Hz PEMF-exposed AMSC-derived exosomes also exhibited a more superior regenerative effect on the osteoarthritic cartilage and ECM synthesis in the rat model of OA.

Previously it has been shown that PEMF could affect biological functions via the production of coherent or interfering fields that modify fundamental electromagnetic fields generated by living organisms.[28] PEMF stimulation could be applied to biological tissues by inductive coupling, which was used to modulate MSCs in the present study.[29,30] Several studies have reported that PEMF could modulate both cell surface receptor expression/activation, and downstream signal transduction pathways, thereby restoring homeostatic cell functions such as viability, proliferation, differentiation, communication with neighboring cells, and interaction with components of ECM.[31,32] It has been postulated that a direct effect of PEMF on phospholipids within the plasma membrane stimulates the production of second messengers, initiating multiple intracellular signal transduction pathways.[33,34] The application of PEMF to MSCs derived from different origins has been shown to modulate the cell cycle and enhance the differentiation.[35-37] In combination with a chondrogenic inductive medium, PEMF stimulation is able to accelerate the hypertrophic cell differentiation, increase the deposition of collagen type I and X, and promote the osteochondral ossification under

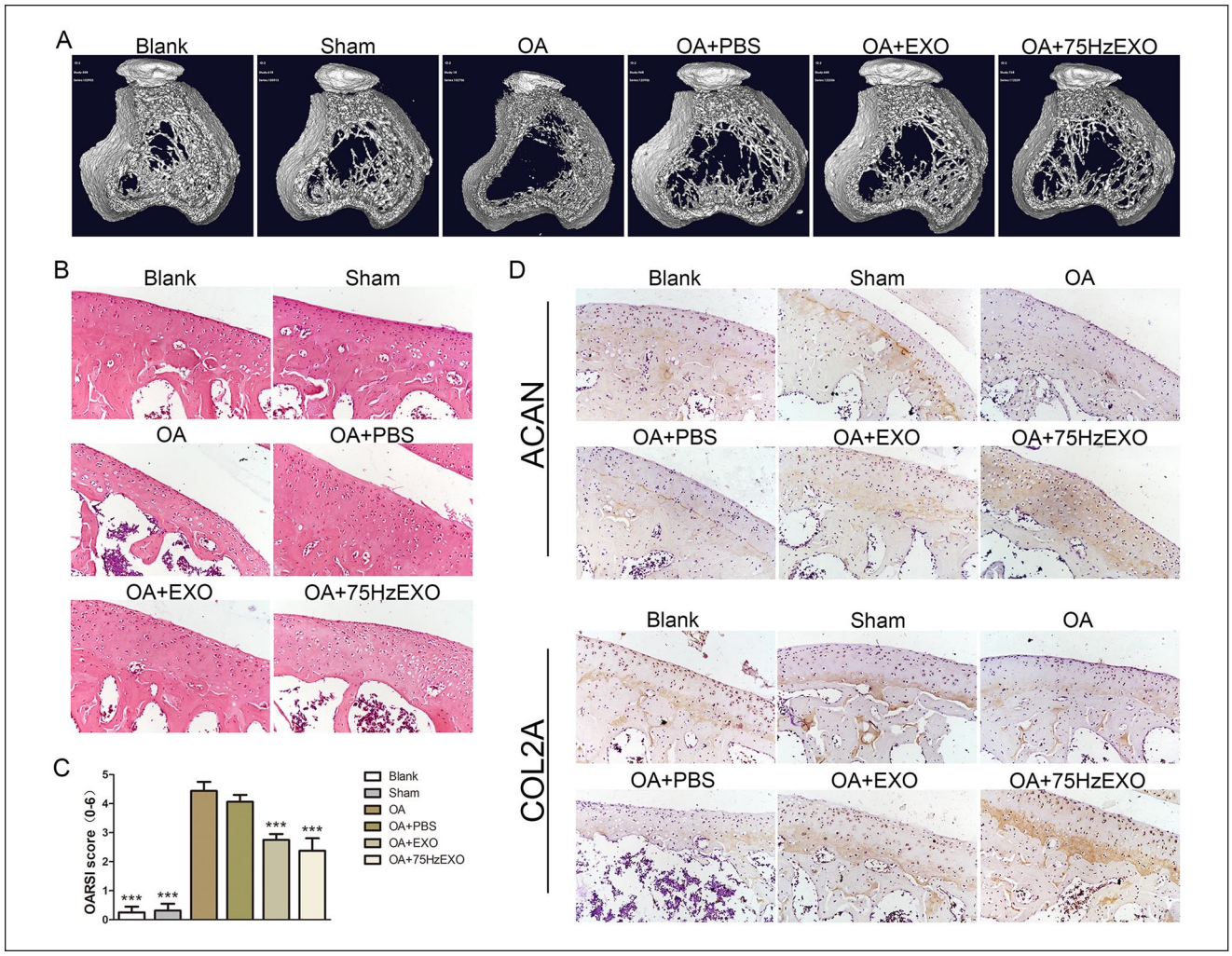

Figure 4. PEMF-regulated AMSC-derived exosomes alleviate cartilage damage in ACLT-induced experimental osteoarthritis rats. (**A**) The micro-CT image of the transverse section of the epiphyseal proximal tibia of rats. (**B**) Images of H&E staining of knee joint specimens. The magnification is 200x. (**C**) OARSI score for the cartilage among different groups. ***<0.001, compared with the OA group. The score was mainly decided according to the cartilage matrix loss and cartilage degeneration observed in the frontal sections.[25] (**D**) Immunohistochemical staining of COL2A1 and ACAN proteins in the cartilage tissue. The magnification is 200x ($n = 3$ for each group).

PEMF = pulsed electromagnetic field; AMSC = adipose tissue derived MSC; ACLT = anterior cruciate ligament transaction; OARSI = Osteoarthritis Research Society International; OA = osteoarthritis.

the 3D culture of rat bone marrow MSCs.[16,23,38] In addition, PEMF could potentiate MSCs' anti-inflammatory responses.[31] In this study, the enhanced effect of PEMF on AMSC-derived exosomes in alleviating inflammation and cartilage degeneration has been demonstrated in the OA rat, which underwent weekly PEMF-exposed AMSC-derived exosome injection for 4 weeks.

Cytokines secreted by immune cells are the main players of OA. IL-1β drives the inflammatory cascade independently or in collaboration with other cytokines, and has been used to trigger inflammation in chondrocyte culture.[39-41] The expression of IL-1β, MMP13, and caspase-1 is elevated in the OA cartilage.[42-45] Varani *et al.*[46] and Ongaro *et al.*[47] reported that at 1.5 mT, the 75-Hz PEMF increased anti-inflammatory properties in chondrocytes via mediating an upregulation of A2A and A3 receptors and inhibiting the release of PGE2, IL-1β, and IL-6 production. Fitzsimmons *et al.*[48] and Tang *et al.*[49] claimed that at 1 mT, the 15-Hz PEMF significantly decreased the production of NO, cGMP, IL-1α, and IL-6 in chondrocytes and vertebral joint cells. These references lead to the conclusion that 15- and 75-Hz PEMFs both have an anti-inflammation effect. However, in consideration of the difference in amplitude of the PEMF, we cannot directly compare the effect of PEMF at 2 different frequencies according to the existing articles. Our previous study stated that PEMF at 75 Hz is superior to

low-frequency PEMF in ameliorating the deterioration of bone microarchitecture in ovariectomized (OVX) mice, and the inhibitory effect of PEMF may be associated with IL-1β inhibition.[31,50] Thus, we designed the experiment that stimulated MSCs with PEMF at an amplitude of 1 mT and a frequency of 15, 45, and 75 Hz respectively. In the present study, the 75-Hz PEMF-exposed AMSC-derived exosomes significantly inhibited IL-1β, MMP13, and caspase-1 levels in the IL-1β-induced chondrocytes. These observations have shown that 75-Hz PEMF stimulation had a superior regulatory effect on AMSC-derived exosomes in relieving the inflammatory responses in OA rats.

Moreover, IL-1β interferes with the production of essential structural proteins, including SOX9, collagen type II, and aggrecan, by influencing the activity of chondrocytes in the joint.[51,52] SOX9 could activate the cartilage ECM genes including COL2A1, COL9A1, and ACAN.[53-55] In the current study, the 75-Hz PEMF-stimulated MSC-derived exosomes obviously promoted the secretion of COL2A1, SOX-9, and ACAN in IL-1β-induced chondrocytes. In addition, the animal study also revealed that the 75-Hz PEMF-stimulated MSC-derived exosomes upregulated COL2A1 and ACAN expression in the cartilage tissue of OA rats. These observations suggested that 75-Hz PEMF-stimulated MSC-derived exosomes could promote chondrocyte matrix synthesis and enhance cartilage repair in OA rats, which were superior to 15- and 45-Hz PEMF-exposed exosomes.

Previously it has been shown that the inflammatory progression of OA could be alleviated by MSCs, which is associated with the multiple miRNAs and long non-coding RNAs (lncRNAs) capsulated in exosomes.[56-60] MSC-derived exosomes can relieve cartilage injury by inhibiting the inflammation and oxidative stress through miR-9-5p[61] and lncRNA MALAT1,[62] and reverse the pathological inflammatory status through miR-21, miR-146a, and miR-181c.[63,64] PEMF has been proved to regulate cellular biological function, activate the intracellular signaling pathways, and affect the mitochondrial energy metabolism. For example, PEMF can induce depolarization in the cell membrane, followed by an increase or decrease in intracellular calcium (Ca^2+). In addition, except for the upregulation of mRNA expressions of Wnt1, Wnt3a, and β-catenin in AMSCs, PEMF intervention could also reduce the expression of dickkopf1 (DKK1) which usually acts as an inhibitor of Wnt signaling pathway.[65,66] In addition, the brief exposure of MSCs to low-amplitude PEMF heightens the anti-inflammatory potential of their exosomes and decreases the expressions of IL-6, Cox-2, and MMP13 in treated chondrocytes, alluding to an enhanced therapeutic application to attenuate cartilage damage in an inflamed articular environment.[23] This current study highlighted the potential role of PEMF in promoting the therapeutic effect of AMSC-derived exosomes, which will open up new direction of research regarding the PEMF-exposed exosome-elicited cartilage regeneration. For instance, PEMF stimulation might upregulate the expression of specific miRNAs in exosomes derived from MSCs, which target signaling pathways, such as Wnt, that affect chondrocyte proliferation, apoptosis, autophagy, or inflammation.

In particular, as demonstrated by Brighton *et al.*,[67] PEMF determines signal transduction through the intracellular release of Ca^{2+}, leading to an increase in cytosolic Ca^{2+} and an increase in activated cytoskeletal calmodulin. Through this mechanism, PEMF modifies some important physiologic parameters of cells, such as proliferation, transduction, transcription, synthesis, and secretion of growth factors.[68,69] However, most of these studies lack homogeneity because they present high variability in terms of magnetic flux density (the component of the magnetic field passing through a surface), signal type, frequency, duration, and the number of treatment sessions. In the present study, we chose the parameters of PEMF based on the previous studies,[16,37,69,70] which showed that PEMF was capable of enhancing the migration of chondrocytes and MSCs as well as modulating the paracrine function of MSCs for the enhancement and re-establishment of cartilage regeneration in states of cellular stress. Despite all these extensive studies, this is one of the first studies which aimed to investigate the possible effects of different frequencies of PEMF on AMSC-derived exosomes. In turn, 75-Hz PEMF was found to be prominent in the regulation of AMSC-derived exosomes in mediating therapeutic effect on OA cartilage.

There are still some limitations to this study. First, on the basis of *in vitro* experiments, 75-Hz PEMF stimulation was found to have superior effect on AMSC-derived exosomes. Thus, in the *in vivo* study, we only verified the regenerative effect of 75-Hz PEMF stimulation in the OA rats but not to compare with those of 15- and 45-Hz PEMFs. The results of this study could lay a foundation for subsequent mechanism exploration. Further studies are needed to investigate the role of miRNA and lncRNAs encapsulated within PEMF-exposed AMSC-derived exosomes and biological secretion of AMSC-derived exosomes in the presence of PEMF stimulation. All these limitations will be addressed in future studies.

Conclusion

In the present study, PEMF-exposed AMSC-derived exosomes could significantly inhibit the degeneration and inflammation of osteoarthritic cartilage. Compared with other frequency parameters, the PEMF at a frequency of 75 Hz showed a superior positive effect on AMSC-derived exosomes in suppressing IL-1β-induced chondrocyte inflammation and ECM catabolism, as well as the

osteoarthritic cartilage degeneration. These findings laid a foundation for the regulatory mechanism of PEMF stimulation on MSC-derived exosomes and opened up a new direction for enhancing the therapeutic effect of MSC-derived exosomes on OA.

Author Contributions

Yang Xu: Conceptualization, Methodology, Data curation, Formal analysis, Writing—original draft, Writing –review & editing. **Qian Wang:** Conceptualization, Methodology, Data curation, Formal analysis, Funding acquisition, Writing—review & editing. **Xiang-Xiu Wang:** Methodology, Investigation, Data curation, Visualization. **Xiao-Na Xiang:** Methodology, Investigation, Data curation, Validation. **Jia-Lei Peng:** Methodology, Investigation, Data curation, Visualization. **Cheng-Qi He:** Conceptualization, Funding acquisition, Supervision, Writing—review & editing. **Hong-Chen He:** Conceptualization, Funding acquisition, Supervision, Writing—review & editing.

Acknowledgments and Funding

The author(s) disclosed receipt of the following financial support for the research, authorship, and/or publication of this article: This work was supported by grants from the National Natural Science Foundation of China, no. 8170226 (Qian Wang).

Declaration of Conflicting Interests

The author(s) declared no potential conflicts of interest with respect to the research, authorship, and/or publication of this article.

Ethical Approval

This study protocol was approved by the Animal Ethics Committee of the West China Hospital of Sichuan University (Sichuan, China; approval no. 2020350A).

ORCID iDs

Cheng-Qi He https://orcid.org/0000-0002-5349-0571
Hong-Chen He https://orcid.org/0000-0003-4635-6769

References

1. O'Neill TW, McCabe PS, McBeth J. Update on the epidemiology, risk factors and disease outcomes of osteoarthritis. Best Pract Res Clin Rheumatol. 2018;32(2):312-26.
2. Vina ER, Kwoh CK. Epidemiology of osteoarthritis: literature update. Curr Opin Rheumatol. 2018;30(2):160-7.
3. Nurul AA, Azlan M, Ahmad Mohd Zain MR, Sebastian AA, Fan YZ, Fauzi MB. Mesenchymal stem cells: current concepts in the management of inflammation in osteoarthritis. Biomedicines. 2021;9(7):785. doi:10.3390/biomedicines9070785.
4. Kwon DG, Kim MK, Jeon YS, Nam YC, Park JS, Ryu DJ. State of the art: the immunomodulatory role of MSCs for osteoarthritis. Int J Mol Sci. 2022;23(3):1618. doi:10.3390/ijms23031618.
5. Bortoluzzi A, Furini F, Scirè CA. Osteoarthritis and its management: epidemiology, nutritional aspects and environmental factors. Autoimmun Rev. 2018;17(11):1097-104.
6. Katz JN, Arant KR, Loeser RF. Diagnosis and treatment of hip and knee osteoarthritis: a review. Jama. 2021;325(6):568-78.
7. Kolasinski SL, Neogi T, Hochberg MC, Oatis C, Guyatt G, Block J, *et al.* 2019 American College of Rheumatology/Arthritis Foundation guideline for the management of osteoarthritis of the hand, hip, and knee. Arthritis Care Res (Hoboken). 2020;72(2):149-62.
8. Fuggle NR, Cooper C, Oreffo ROC, Price AJ, Kaux JF, Maheu E, *et al.* Alternative and complementary therapies in osteoarthritis and cartilage repair. Aging Clin Exp Res. 2020;32(4):547-60.
9. De Bari C, Roelofs AJ. Stem cell-based therapeutic strategies for cartilage defects and osteoarthritis. Curr Opin Pharmacol. 2018;40:74-80.
10. Song Y, Zhang J, Xu H, Lin Z, Chang H, Liu W, *et al.* Mesenchymal stem cells in knee osteoarthritis treatment: A systematic review and meta-analysis. J Orthop Translat. 2020;24:p121-30.
11. Zhang R, Ma J, Han J, Zhang W, Ma J. Mesenchymal stem cell related therapies for cartilage lesions and osteoarthritis. Am J Transl Res. 2019;11(10):6275-89.
12. Bao C, He C. The role and therapeutic potential of MSC-derived exosomes in osteoarthritis. Arch Biochem Biophys. 2021;710:109002.
13. Kim YG, Choi J, Kim K. Mesenchymal stem cell-derived exosomes for effective cartilage tissue repair and treatment of osteoarthritis. Biotechnol J. 2020;15(12):e2000082.
14. Toh WS, Lai RC, Hui JHP, Lim SK. MSC exosome as a cell-free MSC therapy for cartilage regeneration: Implications for osteoarthritis treatment. Semin Cell Dev Biol. 2017;67:56-64.
15. Fuloria S, Subramaniyan V, Dahiya R, Dahiya S, Sudhakar K, Kumari U, *et al.* Mesenchymal stem cell-derived extracellular vesicles: regenerative potential and challenges. Biology (Basel). 2021;10(3):172.
16. Parate D, Franco-Obregón A, Fröhlich J, Beyer C, Abbas AA, Kamarul T, *et al.* Enhancement of mesenchymal stem cell chondrogenesis with short-term low intensity pulsed electromagnetic fields. Sci Rep. 2017;7(1):9421.
17. Succar P, Medynskyj M, Breen EJ, Batterham T, Molloy MP, Herbert BR. Priming adipose-derived mesenchymal stem cells with hyaluronan alters growth kinetics and increases attachment to articular cartilage. Stem Cells Int. 2016;2016:9364213.
18. Rando TA, Ambrosio F. Regenerative rehabilitation: applied biophysics meets stem cell therapeutics. Cell Stem Cell. 2018;22(3):306-9.
19. Thompson WR, Scott A, Loghmani MT, Ward SR, Warden SJ. Understanding mechanobiology: physical therapists as a force in mechanotherapy and musculoskeletal regenerative rehabilitation. Phys Ther. 2016;96(4):560-9.
20. Yang X, He H, Ye W, Perry TA, He C. Effects of pulsed electromagnetic field therapy on pain, stiffness, physical function, and quality of life in patients with osteoarthritis: a systematic review and meta-analysis of randomized placebo-controlled trials. Phys Ther. 2020;100(7):1118-31.

21. Yang X, He H, Zhou Y, Zhou Y, Gao Q, Wang P, *et al.* Pulsed electromagnetic field at different stages of knee osteoarthritis in rats induced by low-dose monosodium iodoacetate: Effect on subchondral trabecular bone microarchitecture and cartilage degradation. Bioelectromagnetics. 2017;38(3):227-38. doi:10.1002/bem.22028.
22. Huang J, Liang Y, Huang Z, Zhao P, Liang Q, Liu Y, *et al.* Magnetic enhancement of chondrogenic differentiation of mesenchymal stem cells. ACS Biomater Sci Eng. 2019;5(5):2200-7.
23. Parate D, Kadir ND, Celik C, Lee EH, Hui JHP, Franco-Obregón A, *et al.* Pulsed electromagnetic fields potentiate the paracrine function of mesenchymal stem cells for cartilage regeneration. Stem Cell Res Ther. 2020;11(1):46.
24. Thomas RG, Unnithan AR, Moon MJ, Surendran SP, Batgerel T, Park CH, *et al.* Electromagnetic manipulation enabled calcium alginate Janus microsphere for targeted delivery of mesenchymal stem cells. Int J Biol Macromol. 2018;110:465-71.
25. Yan B, Liu T, Yao C, Liu X, Du Q, Pan L. LncRNA XIST shuttled by adipose tissue-derived mesenchymal stem cell-derived extracellular vesicles suppresses myocardial pyroptosis in atrial fibrillation by disrupting miR-214-3p-mediated Arl2 inhibition. Lab Invest. 2021;101(11):1427-38.
26. Feng FB, Qiu HY. Effects of Artesunate on chondrocyte proliferation, apoptosis and autophagy through the PI3K/AKT/mTOR signaling pathway in rat models with rheumatoid arthritis. Biomed Pharmacother. 2018;102:1209-20.
27. Gerwin N, Bendele AM, Glasson S, Carlson CS. The OARSI histopathology initiative: recommendations for histological assessments of osteoarthritis in the rat. Osteoarthritis Cartilage. 2010;18(Suppl 3):S24-34.
28. Ross CL, Siriwardane M, Almeida-Porada G, Porada CD, Brink P, Christ GJ, *et al.* The effect of low-frequency electromagnetic field on human bone marrow stem/progenitor cell differentiation. Stem Cell Res. 2015;15(1):96-108.
29. Trock DH. Electromagnetic fields and magnets. Investigational treatment for musculoskeletal disorders. Rheum Dis Clin North Am. 2000;26(1):51-62.
30. Ganesan K, Gengadharan AC, Balachandran C, Manohar BM, Puvanakrishnan R. Low frequency pulsed electromagnetic field: a viable alternative therapy for arthritis. Indian J Exp Biol. 2009;47(12):939-48.
31. Ross CL, Ang DC, Almeida-Porada G. Targeting mesenchymal stromal cells/pericytes (MSCs) with pulsed electromagnetic field (PEMF) has the potential to treat rheumatoid arthritis. Front Immunol. 2019;10:266.
32. Chen CH, Lin Y-S, Fu Y-C, Wang C-K, Wu S-C, Wang G-J, *et al.* Electromagnetic fields enhance chondrogenesis of human adipose-derived stem cells in a chondrogenic microenvironment in vitro. J Appl Physiol (1985). 2013;114(5):647-155.
33. Ceccarelli G, Bloise N, Mantelli M, Gastaldi G, Fassina L, De Angelis MG, *et al.* A comparative analysis of the in vitro effects of pulsed electromagnetic field treatment on osteogenic differentiation of two different mesenchymal cell lineages. Biores Open Access. 2013;2(4):283-94.
34. Ehnert S, van Griensven M, Unger M, Scheffler H, Falldorf K, Fentz A-K, *et al.* Co-culture with human osteoblasts and exposure to extremely low frequency pulsed electromagnetic fields improve osteogenic differentiation of human adipose-derived mesenchymal stem cells. Int J Mol Sci. 2018;19(4):994.
35. Esposito M, Lucariello A, Costanzo C, Fiumarella A, Giannini A, Riccardi G, *et al.* Differentiation of human umbilical cord-derived mesenchymal stem cells, WJ-MSCs, into chondrogenic cells in the presence of pulsed electromagnetic fields. In Vivo. 2013;27(4):495-500.
36. Kaivosoja E, Sariola V, Chen Y, Konttinen YT. The effect of pulsed electromagnetic fields and dehydroepiandrosterone on viability and osteo-induction of human mesenchymal stem cells. J Tissue Eng Regen Med. 2015;9(1):31-40.
37. Kavand H, Haghighipour N, Zeynali B, Seyedjafari E, Abdemami B. Extremely low frequency electromagnetic field in mesenchymal stem cells gene regulation: chondrogenic markers evaluation. Artif Organs. 2016;40(10):929-37.
38. Schwartz Z, Simon BJ, Duran MA, Barabino G, Chaudhri R, Boyan BD. Pulsed electromagnetic fields enhance BMP-2 dependent osteoblastic differentiation of human mesenchymal stem cells. J Orthop Res. 2008;26(9):1250-5.
39. Chow YY, Chin KY. The Role of Inflammation in the Pathogenesis of Osteoarthritis. Mediators Inflamm. 2020;2020:8293921.
40. Kapoor M, Martel-Pelletier J, Lajeunesse D, Pelletier JP, Fahmi H. Role of proinflammatory cytokines in the pathophysiology of osteoarthritis. Nat Rev Rheumatol. 2011;7(1):33-42.
41. Wang MN, Liu L, Zhao L-P, Yuan F, Fu Y-B, Xu X-B, *et al.* [Research of inflammatory factors and signaling pathways in knee osteoarthritis]. Zhongguo Gu Shang. 2020;33(4):388-192.
42. Charlier E, Deroyer C, Ciregia F, Malaise O, Neuville S, Plener Z, *et al.* Chondrocyte dedifferentiation and osteoarthritis (OA). Biochem Pharmacol. 2019;165:49-65.
43. Goldring MB, Otero M. Inflammation in osteoarthritis. Curr Opin Rheumatol. 2011;23(5):471-148.
44. Mehana EE, Khafaga AF, El-Blehi SS. The role of matrix metalloproteinases in osteoarthritis pathogenesis: An updated review. Life Sci. 2019;234:116786.
45. Molla MD, Akalu Y, Geto Z, Dagnew B, Ayelign B, Shibabaw T. Role of Caspase-1 in the pathogenesis of inflammatory-associated chronic noncommunicable diseases. J Inflamm Res. 2020;13:749-64.
46. Varani K, De Mattei M, Vincenzi F, Gessi S, Merighi S, Pellati A, *et al.* Characterization of adenosine receptors in bovine chondrocytes and fibroblast-like synoviocytes exposed to low frequency low energy pulsed electromagnetic fields. Osteoarthritis Cartilage. 2008;16(3):292-304. doi:10.1016/j.joca.2007.07.004.
47. Ongaro A, Varani K, Masieri FF, Pellati A, Massari L, Cadossi R, *et al.* Electromagnetic fields (EMFs) and adenosine receptors modulate prostaglandin E(2) and cytokine release in human osteoarthritic synovial fibroblasts. J Cell Physiol. 2012;227(6):2461-99. doi:10.1002/jcp.22981.
48. Fitzsimmons RJ, Gordon SL, Kronberg J, Ganey T, Pilla AA. A pulsing electric field (PEF) increases human chondrocyte proliferation through a transduction pathway involving nitric oxide signaling. J Orthop Res. 2008;26(6):854-9. doi:10.1002/jor.20590.
49. Tang X, Alliston T, Coughlin D, Miller S, Zhang N, Waldorff EI, *et al.* Dynamic imaging demonstrates that pulsed electro-

magnetic fields (PEMF) suppress IL-6 transcription in bovine nucleus pulposus cells. J Orthop Res. 2018;36(2):778-87. doi:10.1002/jor.23713.
50. Wang L, Li Y, Xie S, Huang J, Song K, He C. Effects of pulsed electromagnetic field therapy at different frequencies on bone mass and microarchitecture in osteoporotic mice. Bioelectromagnetics. 2021;42(6):441-54. doi:10.1002/bem.22344.
51. Jenei-Lanzl Z, Meurer A, Zaucke F. Interleukin-1β signaling in osteoarthritis: chondrocytes in focus. Cell Signal. 2019;53:212-23.
52. Vincent TL. IL-1 in osteoarthritis: time for a critical review of the literature. F1000res. 2019;8:934.
53. Bridgewater LC, Lefebvre V, de Crombrugghe B. Chondrocyte-specific enhancer elements in the Col11a2 gene resemble the Col2a1 tissue-specific enhancer. J Biol Chem. 1998;273(24):14998-5006.
54. Kiani C, Chen L, Wu YJ, Yee AJ, Yang BB. Structure and function of aggrecan. Cell Res. 2002;12(1):19-32.
55. Lian C, Wang X, Qiu X, Wu Z, Gao B, Liu L, *et al.* Collagen type II suppresses articular chondrocyte hypertrophy and osteoarthritis progression by promoting integrin β1-SMAD1 interaction. Bone Res. 2019;7:8.
56. Jin Z, Ren J, Qi S. Human bone mesenchymal stem cells-derived exosomes overexpressing microRNA-26a-5p alleviate osteoarthritis via down-regulation of PTGS2. Int Immunopharmacol. 2020;78:105946.
57. Li H, Guan SB, Lu Y, Wang F. MiR-140-5p inhibits synovial fibroblasts proliferation and inflammatory cytokines secretion through targeting TLR4. Biomed Pharmacother. 2017;96:208-14.
58. Meng F, Li Z, Zhang Z, Yang Z, Kang Y, Zhao X, *et al.* MicroRNA-193b-3p regulates chondrogenesis and chondrocyte metabolism by targeting HDAC3. Theranostics. 2018;8(10):2862-83.
59. Tao SC, Yuan T, Zhang YL, Yin WJ, Guo SC, Zhang CQ. Exosomes derived from miR-140-5p-overexpressing human synovial mesenchymal stem cells enhance cartilage tissue regeneration and prevent osteoarthritis of the knee in a rat model. Theranostics. 2017;7(1):180-95.
60. Wu MH, Tsai C-H, Huang Y-L, Fong Y-C, Tang C-H. Visfatin promotes IL-6 and TNF-α production in human synovial fibroblasts by repressing miR-199a-5p through ERK, p38 and JNK signaling pathways. Int J Mol Sci. 2018;19(1):190.
61. Jin Z, Ren J, Qi S. Exosomal miR-9-5p secreted by bone marrow-derived mesenchymal stem cells alleviates osteoarthritis by inhibiting syndecan-1. Cell Tissue Res. 2020;381(1):99-114.
62. Liu Y, Zou R, Wang Z, Wen C, Zhang F, Lin F. Exosomal KLF3-AS1 from hMSCs promoted cartilage repair and chondrocyte proliferation in osteoarthritis. Biochem J. 2018;475(22):3629-38.
63. Ti D, Hao H, Fu X, Han W. Mesenchymal stem cells-derived exosomal microRNAs contribute to wound inflammation. Sci China Life Sci. 2016;59(12):1305-12.
64. Wang Y, Shen S, Li Z, Li W, Weng X. MIR-140-5p affects chondrocyte proliferation, apoptosis, and inflammation by targeting HMGB1 in osteoarthritis. Inflamm Res. 2020;69(1):63-73.
65. Yuan J, Xin F, Jiang W. Underlying signaling pathways and therapeutic applications of pulsed electromagnetic fields in bone repair. Cell Physiol Biochem. 2018;46(4):1581-94.
66. Ross CL, Zhou Y, McCall CE, Soker S, Criswell TL. The use of pulsed electromagnetic field to modulate inflammation and improve tissue regeneration: a review. Bioelectricity. 2019;1(4):247-59.
67. Brighton CT, Wang W, Seldes R, Zhang G, Pollack SR. Signal transduction in electrically stimulated bone cells. J Bone Joint Surg Am. 2001;83(10):1514-23.
68. Aaron RK, Boyan BD, Ciombor DM, Schwartz Z, Simon BJ. Stimulation of growth factor synthesis by electric and electromagnetic fields. Clin Orthop Relat Res. 2004;419:30-7.
69. de Girolamo L, Stanco D, Galliera E, Viganò M, Colombini A, Setti S, *et al.* Low frequency pulsed electromagnetic field affects proliferation, tissue-specific gene expression, and cytokines release of human tendon cells. Cell Biochem Biophys. 2013;66(3):697-708.
70. Hopper RA, VerHalen JP, Tepper O, Mehrara BJ, Detch R, Chang EI, *et al.* Osteoblasts stimulated with pulsed electromagnetic fields increase HUVEC proliferation via a VEGF-A independent mechanism. Bioelectromagnetics. 2009;30(3):189-97.